smaller than the value used here, gave ΔH_f° = 61.5 kcal/mol for coronene vs 67.8 kcal/mol reported here.

Acknowledgment. This research was supported, in part, by Grants 668248, 669274 and 662286 of the PSC-CUNY Research Award Program of the City University of New York and a grant of computing time from the City University Committee on Research Computing. We thank Prof. W. F. Berkowitz for performing the MMX calculation on coronene.

Registry No. C_6H_6, 71-43-2; phenanthrene, 85-01-8; pyrene, 129-00-0; triphenylene, 217-59-4; benzo[*e*]pyrene, 192-97-2; perylene, 198-55-0; benzo[*ghi*]perylene, 191-24-2; coronene, 191-07-1; circumcoronene, 72210-95-8.

Rubber-Rubber Adhesion with Connector Molecules

E. Raphaël and P. G. de Gennes*

Collège de France, 75231 Paris Cedex 05, France *(Received: September 30, 1991)*

We consider two rubber blocks A and B in close contact, with some extra A chains (connectors) bound to the surface of the B block and entering freely in the A block. The connectors are assumed not to break, but to slip out by a viscous process when the two blocks are separated. In that model, the adhesion energy has two sources: the thermodynamic work W of Dupré, and the suction work required to pull out the connectors. We show that these two contributions are not simply additive. Our main practical result is to predict the minimum number ρ (per unit area) or the minimum length N of the connectors required to enhance significantly the adhesion energy.

I. Introduction

When attempting to bridge the gap between polymer science and fracture mechanics, it is sometimes useful to focus on *weak mechanical junctions*.[1,2] When a fracture propagates along such a junction, the dissipation tends to be localized in a *thin sheet* near the fracture plane, in contrast with the cohesive rupture of polymers.[3]

Figure 1 shows an example of a weak rubber (A)/rubber (B) junction. The interface between the two rubber blocks is strengthened by grafting some A polymer chains (adhesion promoters) to the B block. We call them the *connectors*. [In order to avoid complicated zigzags of the promoters between the two sides of the junction, we assume the two polymers (A) and (B) to be incompatible: then the connectors seldom (if ever) enter the B region].

The aim of the present study is to analyze the steady-state propagation of a crack along the junction displayed on Figure 1, in the limit of *low fracture velocities*. In particular, we want to discuss the interplay between (i) the cohesion due to capillary forces and (ii) the adhesion orginating from the pull-out of the promoters.

The paper is organized as follows. In section II.1, we consider the behavior of a single promoter in air. We then evaluate the threshold stress σ^* required to separate the two rubber blocks (section II.2). When $\sigma > \sigma^*$, the system cannot withstand the applied stress any more and starts to open: the connectors become progressively sucked out of the A region. This suction process is analyzed in section II.3. The last part of the paper (sections III.1, III.2, and III.3) is devoted to the elastic field around the junction.

For technical simplicity, we assume that the two rubbers have the same elastic properties (same Young modulus (E) and Poisson ratio ($\nu \sim 1/2$)). All our analysis is restricted to scaling laws: the exact prefactors in our formulas remain unknown.

II. The Constitutive Model

Before considering the propagation of a fracture along a rubber (A)/rubber (B) interface, we first discuss what happens when the two rubber blocks are submitted to a uniform tensile stress σ (Figure 2). In particular, we want to calculate (a) the threshold stress σ^* required to separate the two blocks, (b) the friction constant Q characterizing the "suction" process which occurs when $\sigma > \sigma^*$, and (c) the terminal opening h_f.

II.1. A Single Promoter in Air. The situation is described on Figure 3. The two blocks A and B have been separated by an air gap of thickness h. A connector bridges this gap: the bridging portion contains a certain number of monomers (n). We do not, for the moment, assume that the bridge is fully stretched.

We describe the bridge as a "pillar" of diameter d and height h. The volume fraction in the pillar is

$$\phi \cong na^3/d^2h \tag{2.1}$$

Our model[4] describes the polymer inside the pillar as a semidilute solution in a poor solvent which is just in equilibrium with the solvent.[5] For such a solution, the correlation length is $\xi = a/\phi$ and the interfacial energy with the solvent is

$$\gamma_A \cong kT/\xi^2 \tag{2.2}$$

We shall often use, instead of γ_A, the dimensionless parameter:

$$K_A \equiv \frac{\gamma_A a^2}{kT} \cong \frac{a^2}{\xi^2} \cong \phi^2 \tag{2.3}$$

Small values of K_A mean θ solvents. The realistic situation with air (a very bad solvent !) is $K_A \sim 1$. But we focus our attention on small values of K_A for three reasons: (a) they may be of interest when we fracture in a liquid and not in air; (b) the discussion gives more insight; (c) in any case, the limit $K_A \sim 1$ for air may still be taken on our scaling formulas without harm.

Let us now discuss the pulling force f necessary to maintain the pillar in Figure 3. This is a combination of two terms:

a capillary force:

$$f_c = \gamma_A \pi d \quad (\sim \gamma_A d) \tag{2.4}$$

an elastic force which in our case has the ideal chain form:

$$f_{el} \cong kT\frac{h}{na^2} \cong kT\frac{a}{d^2\phi} \tag{2.5}$$

(1) de Gennes, P. G. *J. Phys. Fr.* **1989**, *50*, 2551.
(2) de Gennes, P. G. *C.R. Acad. Sci. (Pairs) 2* **1989**, *309*, 1125.
(3) Kinloch, A. J.; Young, R. J. *Fracture Behavior of Polymers*; Elsevier: New York, 1983.
(4) A somewhat related analysis concerning the deformation behavior of a collapsed coil in a poor solvent may be found in: Halperin, A.; Zhulina, E. B. *Europhys. Lett.* **1991**, *15*, 417.
(5) de Gennes, P. G. *J. Phys. Lett. (Paris)* **1978**, *39*, L 299.

0022-3654/92/2096-4002$03.00/0

The minimum of $f = f_c + f_{el}$ is reached when

$$K_A\phi\frac{d^3}{a^3} \simeq 1 \tag{2.6}$$

or equivalentely (from eq 2.3)

$$d \simeq a\phi^{-1} \simeq \xi \tag{2.7}$$

The corresponding value of the force is

$$f^* \simeq \frac{kT}{a}K_A^{1/2} \tag{2.8}$$

This is the threshold force required to pull out one connector.

II.2. The Threshold Stress. Suppose that a uniform stensile stress σ is applied to the rubber blocks (Figure 2). The energy g per unit area (as a function of the distance h between the two blocks) has the aspect shown on Figure 4, where W denotes the Dupré work of separation of the two rubbers *in the absence of promoter*:

$$W = \gamma_A + \gamma_B - \gamma_{AB} \tag{2.9}$$

For $h > a$, the energy $g(h)$ is linear (see eq 2.8):

$$g(h) \simeq \left[\frac{kT}{aD^2}K_A^{1/2} - \sigma\right]h + (\text{const}) \qquad (h > a) \tag{2.10}$$

As long as σ is smaller than the critical value

$$\sigma^* \simeq \frac{kT}{aD^2}K_A^{1/2} \tag{2.11}$$

the energy $g(h)$ is minimal for $h = 0$ and the system remains closed. But as soon as σ becomes greater than σ^*, the energy minimum is not at $h = 0$. It is true that there remains an energy *barrier*: but, in the fracture processes to be discussed below, the fracture tip acts as a nucleation center and removes this barrier. Thus σ^* appears as a threshold stress for opening. When $\sigma > \sigma^*$, the promoters are progressively sucked out of the rubber A. This suction process ends only when all the promoter is extracted, i.e., for $h = h_f$ with

$$h_f \simeq aNK_A^{1/2} \tag{2.12}$$

Here N is the polymerization index of the promoter. We now analyze the dissipation involved in this suction process.

II.3. The Suction Process. Assume that $\sigma > \sigma^*$. When the distance between the two rubber blocks increases by dh, the chain is sucked by a length

$$ds = K_A^{-1/2}\,dh \tag{2.13}$$

The work performed by the stress σ is the sum of two terms:

$$\sigma\,dh = \frac{1}{D^2}\frac{\partial}{\partial h}\left(\frac{kT}{a}K_A^{1/2}h\right)dh + \rho f_v\,ds \tag{2.14}$$

The first term is the work of extraction of the connectors. The second term represents the viscous losses inside the rubber, due to slippage of the connector chains. In the simplest picture

$$f_v = \zeta_t\frac{ds}{dt} \tag{2.15}$$

where $\zeta_t \simeq \zeta_1 N$ is a tube friction coefficient (we ignore for the moment the complications related to the fact that when the connector is half pulled out, the friction is also reduced by a factor 1/2).

Equations 2.14 and 2.15 give us a suction law of the form

$$Q\frac{dh}{dt} = \sigma - \sigma^* \tag{2.16}$$

where $Q = \rho\zeta_t K_A^{-1}$ is the friction coefficient of the junction and is, for the moment, taken to be independent of h.

III. Fracture

III.1. General Features. We now consider the propagation of a fracture along the rubber (A)/rubber (B) interface. The general aspect of the junction is shown on Figure 5. Following ref 6, we describe the elastic field associated with the junction by a superposition $\phi(x)$ of elementary sources extending over all the active part of the junction (i.e., from $I(x=0)$ to $J(x=L)$). The normal stress distribution $\sigma(x)$ and the crack opening $h(x)$ are then given by

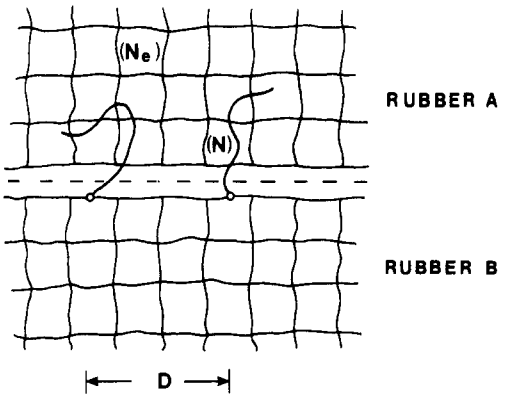

Figure 1. A model for a weak rubber (A)/rubber (B) junction. The two parts are connected by long A polymer chains (adhesion promoters) grafted to the network B and entering freely in the A block.

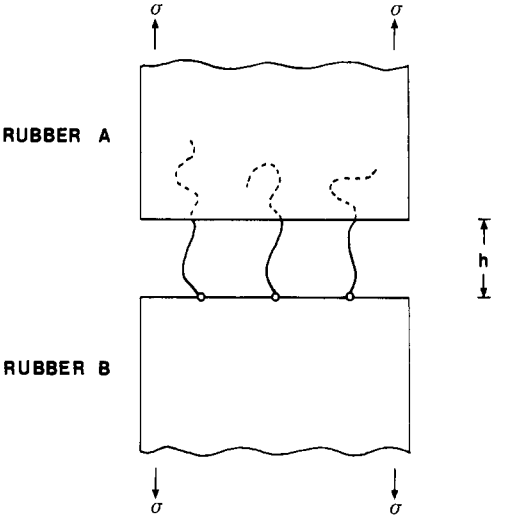

Figure 2. The two rubber blocks submitted to a uniform tensile stress σ.

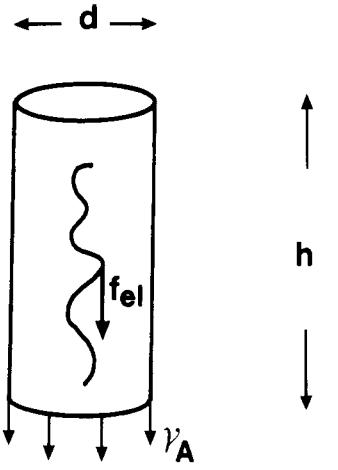

Figure 3. A connector bridging the air gap (of thickness h) between the two blocks A and B. We describe the bridge as a "pillar" of diameter d and height h. The pulling force necessary to maintain the pillar is a combination of a capillary force $f_c \sim \gamma_A\pi d$ and an elastic force f_{el}.

(6) de Gennes, P. G. *Can. J. Phys.* **1990**, *68*, 1049.

$$\sigma(x) = \begin{cases} 0 & (x < 0) \\ \mu \int_0^x dy\, \phi(y)(x - y)^{-1/2} & (x > 0) \end{cases} \quad (3.1)$$

$$h(x) = \begin{cases} 2(1-\nu) \int_x^L dy\, \phi(y)(y - x)^{1/2} & (x < L) \\ 0 & (x > L) \end{cases} \quad (3.2)$$

(We assume a mode I plane strain loading.[7])

At large distances ($|x| \gg L$), the eqs 3.1 and 3.2 reduce to the standard scaling laws for a crack in a purely elastic medium:[7]

$$\sigma(x) = K(2\pi x)^{-1/2} \qquad (x \gg L) \quad (3.3)$$

$$h(x) = 2(1 - \nu)\frac{K}{\mu}\left(\frac{|x|}{2\pi}\right)^{1/2} \qquad (-x \gg L) \quad (3.4)$$

with

$$(2\pi)^{-1/2} K \mu^{-1} = \int_0^L dy\, \phi(y) \quad (3.5)$$

where $\mu = E/2(1 + \nu)$ is the shear modulus and K is called the stress intensity factor.

We now impose the suction law (2.16) in all the active region IJ (apart from a narrow region of size $\sim a$ near the tip (J) of the junction). Assuming a steady-state propagation of the fracture (velocity V), we obtain

$$\mu^{-1}\sigma(x) - \mu^{-1}\sigma^* = \lambda \frac{dh}{dx} \qquad (0 < x < L - a) \quad (3.6)$$

where λ is defined by

$$\lambda = (1 - \nu)\frac{QV}{\mu} = \frac{V}{V^*} \quad (3.7)$$

Equation 3.6 must be supplemented by the boundary condition:

$$h(x=0) = h_f \quad (3.8)$$

where h_f is the terminal value of the junction opening (eq 2.12).

III.2. Distribution of Sources. The distribution of sources $\phi(x)$ can be written as the sum of two contributions: (a) the "initiation distribution" $\phi_{ini}(x)$ determined in the Appendix 1 and corresponding to the elastic field in the absence of connectors; (b) a (yet unknown) "viscous distribution" $\phi_{vis}(x)$ associated with the suction process:

$$\phi(x) = \phi_{ini}(x) + \phi_{vis}(x) \quad (3.9)$$

Accordingly, the stress $\sigma(x)$ and the "density of dislocations" $-dh/dx$ can be written as

$$\sigma(x) = \sigma_{ini}(x) + \sigma_{vis}(x) \quad (3.10)$$

$$-\frac{dh}{dx} = -\frac{dh_{ini}}{dx} - \frac{dh_{vis}}{dx} \quad (3.11)$$

Since $\sigma_{ini}(x) = 0$ for $x < L - a$ (see Appendix 1), eq 3.6 reduces to

$$\mu^{-1}\sigma_{vis}(x) - \mu^{-1}\sigma^* = -\lambda\frac{dh_{vis}}{dx} - \lambda\frac{dh_{ini}}{dx} \qquad (0 < x < L - a) \quad (3.12)$$

Our aim is to find a function $\phi_{vis}(x)$ satisfying eq 3.12. Put

$$\phi_{vis}(x) = \phi_H(x) + \phi_{per}(x) \quad (3.13)$$

which $\phi_H(x)$ satisfies

$$\mu^{-1}\sigma_H(x) - \mu^{-1}\sigma^* = -\lambda\frac{dh_H}{dx} \qquad (0 < x < L - a) \quad (3.14)$$

$$\sigma_H(x = L - a) = \sigma^* \quad (3.15)$$

(7) Kanninen, M.; Popelar, C. *Advanced Fracture Mechanics*; Oxford University Press: London, 1985.

Figure 4. Energy (per unit area) versus gap for the system depicted in Figure 2.

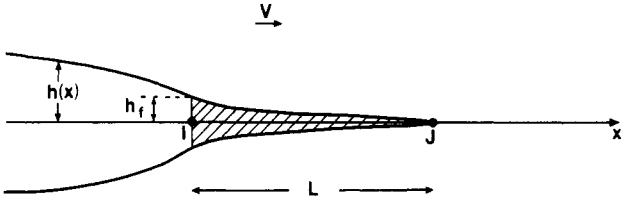

Figure 5. A global view of the advancing fracture. The junction corresponds to the interval IJ.

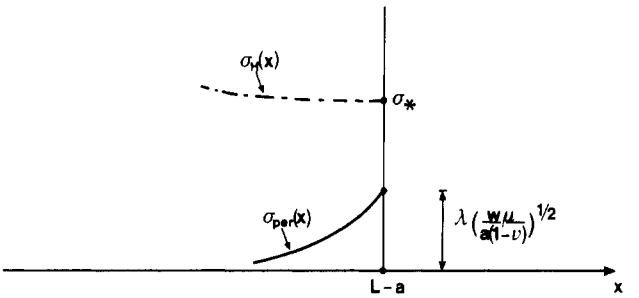

Figure 6. Schematic plot of the stress distribution $\sigma_H(x)$ and $\sigma_{per}(x)$ for $x \lesssim L - a$.

and $\phi_{per}(x)$ is a perturbation. The system (3.14, 3.15) has been solved recently by Hui et al. in their thorough investigation of cohesive zone models.[8] The result is

$$\phi_H(x) = \mu^{-1}\sigma^* \frac{\cos \pi\epsilon}{\pi} x^{-(1/2+\epsilon)}[(L - a) - x]^{\epsilon} \qquad (0 < x < L - a)$$

$$= 0 \qquad \text{(otherwise)} \quad (3.16)$$

with

$$\tan(\pi\epsilon) = \lambda \quad (3.17)$$

Inserting eq 3.14 into eq 3.12, we get

$$\mu^{-1}\sigma_{per}(x) = -\lambda\frac{dh_{per}}{dx} - \lambda\frac{dh_{ini}}{dx} \qquad (0 < x < L - a) \quad (3.18)$$

Suppose that

$$-\frac{dh_{per}}{dx} \gg -\frac{dh_{ini}}{dx} \quad (3.19)$$

Then

$$\mu^{-1}\sigma_{per}(x) \simeq -\lambda\frac{dh_{ini}}{dx}$$

$$\simeq \lambda\left(\frac{W}{\mu(1-\nu)}\right)^{1/2}(L - x)^{-1/2} \quad (0 < x < L - a) \quad (3.20)$$

Within the range $(0, L - a)$, the function $\mu^{-11}\sigma_{per}(x)$ is then maximal for $x = L - a$:

(8) Hui, C.; Xu, D. B.; Fager, L. O.; Bassani, J. L., to be published.

$$\max_{(0,L-a)} \mu^{-1}\sigma_{per}(x) \simeq \lambda\left(\frac{W}{a\mu(1-\nu)}\right)^{1/2} \quad (3.21)$$

As long as λ is smaller than a certain critical value

$$\lambda_c \simeq \frac{\mu^{-1}\sigma_H(x = L-a)}{\left(\frac{W}{a\mu(1-\nu)}\right)^{1/2}} \quad (3.22)$$

the function $\mu^{-1}\sigma_{per}(x)$ satisfies (see Figure 6)

$$\mu^{-1}\sigma_{per}(x) \ll \mu^{-1}\sigma_H(x) \quad (3.23)$$

and thus $\phi_{vis}(x)$ differs only slightly from $\phi_H(x)$. [One may wonder whether eq 3.20 is consistent with the initial assumption (3.19). This problem will be discussed in the Appendix 2.]

For a rubbery material, the shear modulus μ is of order

$$\mu \approx kT/N_e a^3 \quad (3.24)$$

where N_e is the average number of monomers between cross-links in the bulk rubber. Inserting eqs 3.15 and 3.24 into eq 3.22, we arrive at

$$\lambda_c = (\text{const})N_e^{1/2}(D/a)^{-2}(W/\gamma_A)^{-1/2} \quad (3.25)$$

III.3. Mechanical Behavior of the Junction: The Slow Regime. In all what follows we shall assume that $\lambda \ll \lambda_c$ (slow regime). The distribution of sources can then be approximately written as (see section III.2):

$$\phi(x) \simeq \phi_{ini}(x) + \phi_H(x) \quad (3.26)$$

where ϕ_{ini} and ϕ_H are respectively given by (A1.4) and (3.16). The length L of the junction is determined by the boundary condition:

$$h_f = \int_0^L dy\ \phi(y) y^{-1/2} \quad (3.27)$$

Using eq 3.26, we get

$$h_f \simeq \left(\frac{W}{\mu(1-\nu)}\right)^{1/2} L^{1/2} + \frac{\cos \pi\epsilon}{\pi}\Gamma(1-\epsilon)\,\Gamma(1+\epsilon)\mu^{-1}\sigma^*(L-a) \quad (3.28)$$

where $\Gamma(x)$ denotes the gamma function. Taking into account that in the slow regime the parameter ϵ (eq. (3.17)) satisfies $\epsilon \ll 1$, and omitting all numerical prefactors, we get

$$L + \alpha^{1/2}L^{1/2} = L_0 \quad (3.29)$$

with

$$L_0 = \mu h_f/\sigma^* \quad (3.30)$$

and

$$\alpha = \frac{W\mu}{(\sigma^*)^2(1-\nu)} \quad (3.31)$$

Thus the length L of the junction is given by

$$L = \frac{1}{4}\alpha\left[\left(1 + 4\frac{L_0}{\alpha}\right)^{1/2} - 1\right]^2 \quad (3.32)$$

and has the following limiting behaviors:

$$L \simeq \begin{cases} \frac{L_0^2}{\alpha}\left[1 - 2\left(\frac{L_0}{\alpha}\right) + \dots\right] & (L_0 \ll \alpha) \\ L_0\left[1 - \left(\frac{\alpha}{L_0}\right)^{1/2} + \dots\right] & (L_0 \gg \alpha) \end{cases} \quad (3.33)$$

Note that, in the regime $L_0 \ll \alpha$, the length of the junction is much smaller than L_0. We now consider the stress intensity factor (3.5). Using eq 3.26, we obtain

$$K \simeq \left(\frac{\mu W}{(1-\nu)}\right)^{1/2} + \mu^{-1}\sigma^* L^{1/2} \simeq \left(\frac{\mu W}{(1-\nu)}\right)^{1/2}\left(\frac{L_0}{L_0 - L}\right) \quad (3.34)$$

The fracture energy G may then be deduced from the Irwin equation[7]

$$G = \frac{(1-\nu)}{2\mu}K^2 \quad (3.35)$$

The result is

$$G \simeq W\left(\frac{L_0}{L_0 - L}\right)^2 \quad (3.36)$$

and the limiting behaviors are

$$G \simeq \begin{cases} W\left[1 + 2\left(\frac{L_0}{\alpha}\right) + \dots\right] & (L_0 \ll \alpha) \\ \sigma^* h_f(1-\nu)\left[1 + \left(\frac{\alpha}{L_0}\right)^{1/2} + \dots\right] & (L_0 \gg \alpha) \end{cases} \quad (3.37)$$

When $L_0 \ll \alpha$, the connectors are unimportant, and the adhesion energy reduces to the thermodynamic work W. When $L_0 \gg \alpha$, the connectors are dominant, and the adhesion energy is proportional to the product $\sigma^* h_f$. σ^* is independent of the length N of the connectors, but proportional to their number density ρ (eq 2.11). On the other hand, h_f is independent of ρ, but proportional to N (eq 2.12).

The main interest of our discussion is to show how, for intermediate situations with $L_0 \sim \alpha$, the two contributions are superposed: they do not add simply, as it is clear from eqs 3.36 and 3.32.

For instance, note that in the regime $L_0 > \alpha$ (i.e., $\sigma^* h_f > W$), the leading correction to $\sigma^* h_f$ is $(W\sigma^* h_f)^{1/2}$ (rather than W). Thus, in this regime, the fracture energy cannot simply be written as $G = \sigma^* h_f + W$.

IV. Conclusions

1. Relative Role of the Pull Out ($\sigma^* h_+$) and Capillary Adhesion (W). Within the framework of the model discussed in section II, the quantities σ^* and h_f are given respectively by eqs 2.11 and 2.12. The essential parameter is the ratio

$$\frac{L_0}{\alpha} \cong \frac{h_f\sigma^*}{W} \cong N\left(\frac{a}{D}\right)^2\frac{\gamma_A}{W} \quad (4.1)$$

The limiting behaviors (3.33) and (3.37) can be rewritten as

$$L \simeq \begin{cases} a\,\frac{N^2}{N_e}\,(W/\gamma_A)^{-1} & (N \ll N_c) \\ a\,\frac{N}{N_e}\left(\frac{D}{a}\right)^2 & (N \gg N_c) \end{cases} \quad (4.2)$$

$$G \cong \begin{cases} W & (N \ll N_c) \\ \gamma_A N (D/a)^{-2} & (N \gg N_c) \end{cases} \quad (4.3)$$

with

$$N_c \simeq (D/a)^2(W/\gamma_A) \quad (4.4)$$

Thus, as long as the polymerization index N of the connectors is smaller than the critical value N_c (eq 4.4), the main contribution to the fracture energy comes from the capillary forces: $G \simeq W$ (independent of N). When $N \gg N_c$, the dissipation associated with the suction process dominates and $G \simeq \sigma^* h_f \simeq \gamma_A(D/a)^{-2}N$. Uusually, the energies W and γ_A are of the same order of magnitude and thus $N_c \sim (D/a)^2$. Since (in the limit of low surface

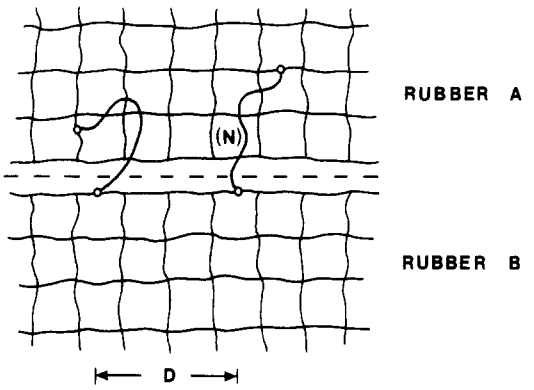

Figure 7. A model for a weak rubber (A)/rubber (B) junction. Here the connectors are chemically attached at both ends.

density ρ) each promoter occupies roughly a half-sphere with a radius $R \sim aN^{1/2}$, the crossover regime $N \sim N_c$ corresponds to the overlap of the different promoters.

2. Comparison between Pull Out and Chemical Bridging. (a) We discussed connectors which are grafted on one block and are free at the other end (Figure 1): they can thus be pulled out without any chemical rupture. This gave us an adhesion energy (for $N > N_c$).

$$G \cong \sigma^* h_f \approx \frac{NkT}{D^2} K_A \tag{4.5}$$

$$\approx \frac{Na^2}{D^2}\gamma_A \approx \frac{R_0^2}{D^2}\gamma_A \tag{4.6}$$

where we made use of eqs 2.3. R_0 is the original radius of gyration of the connector coils.

Consider now the (realistic) limit where air is a very bad solvent for the connectors. Then $\gamma_A a^2 \sim U_v$, a typical van der Waals energy between two adjacent monomers, and we may write

$$G_{\text{pull out}} \sim (N/D^2)U_v \tag{4.7}$$

(b) Let us now compare this prediction to what we have for another physical situation, where each connector is now chemically attached at both ends (Figure 7). In this case scission must take place, and the resulting fracture energy can be estimated from the classical argument of Lake and Thomas.[9] At the moment of rupture, *each* monomer along one connector has stored an energy comparable to the chemical bond energy U_χ. When rupture takes place on one of them, the energy stored in *all* the N monomers is dissipated into heat. Thus

$$G_{\text{scission}} \sim (N/D^2)U_\chi \tag{4.8}$$

And we arrive at the following prediction:

$$\frac{G_{\text{scission}}}{G_{\text{pull out}}} \cong \frac{U_\chi}{U_v} \tag{4.9}$$

In a few cases, such as ref 10, the effects of adhesion promoters which are either free at one end or bound at both ends have been compared experimentally. The bound case gives stronger adhesion, but not by a factor as large as expected from (4.9). However, this is not totally surprising: the connectors which were used in these experiments were short ($N < 20$) and made very compact structures, which have nothing to do with our long, loose, connectors.

3. Other, Related, Weak Junctions. Our analysis of the elastic field around the junction (section III) is independent of the constitutive model developed in section II. Thus, the fundamental forms (3.32) and (3.36) should retain their meanings for other weak mechanical junctions (e.g., at the interface between two glassy polymers A and B with a monolayer of AB copolymer, if the copolymer is extracted by suction and does not break. This, however, appears to be a rare event.[11]

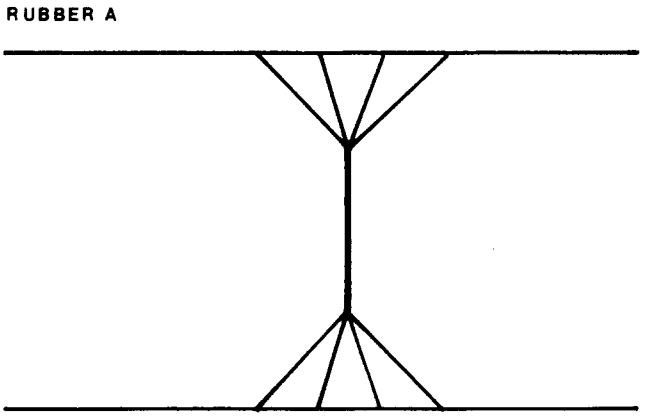

Figure 8. A "bundle" resulting from the association of four connectors.

4. Technical Points. (a) The explicit expressions of σ^*, h_f, and Q, derived in section II, are based on a specific model. It was assumed in particular that the promoters never enter the lower part of the junction. This excludes the case of a rubber (A)/rubber (A) interface, where the promoters (A polymer chains) perform complicated zigzags between the two sides of the junction. This "many-stitch problem" is currently being studied by Hong.

(b) The friction constant $Q = \rho\zeta_t K_A^{-1}$ derived in section II.3 is very different from the expression $Q = \zeta_t/\rho a^4$ proposed in ref 1. While the former is proportional to the number ρ of promoters per unit area, the latter varies as ρ^{-1}. The origin of this discrepancy is the following. In ref 1, no value dilatation between point I and point J was allowed: all the junction volume was filled up with polymer. Here we assume that an extracted connector is exposed to the air. What really happens in nature could however be more complex. Since individual promoters are unhappy when exposed to the air, they might tend to gather to form "bundles" (Figure 8). This process will be discussed in a separate publication.

(c) Our description of the adhesive failure of the junction has been restricted to slow velocities ($\lambda \ll \lambda_c$). In this regime, the force exerted on one connector is of order $\sigma^* D^2 \sim kT/a$, and is therefore much smaller than the critical force corresponding to chemical rupture.

(d) As discussed in ref 1, an improved version of the mechanical equation (2.16) is

$$\frac{h_f - h}{h_f}\frac{dh}{dt} = Q^{-1}(\sigma - \sigma^*) \tag{4.10}$$

where the factor $(h_f - h)/h_f$ expresses the fact that the suction process becomes easier when only a small portion of the promoter length remains to be sucked out. Equation 4.10 will require a separate study.

Appendix 1. The Initiation Distribution

In this appendix, we consider the elastic field associated with the rubber (A)/rubber (B) junction in the absence of promoter. Far from the fracture tip (J), we expect the normal stress to be given by the standard scaling law:

$$\sigma \simeq K(x - L)^{-1/2} \tag{A1.1}$$

Since in the absence of promoter the fracture energy G reduces to W (eq 2.9), the Irwin relation (3.35) yields

$$K \simeq \left(\frac{W\mu}{(1-\nu)}\right)^{1/2} \tag{A1.2}$$

At some place ($x = x_{\min}$) near the fracture tip, the form A1.1 (which assumes the rubber to be a linear elastic material) ceases

(9) Lake, G. J.; Thomas, A. G. *Proc. Soc. London, Ser. A* **1967**, *300*, 108.
(10) Plueddemann, E.; Collins, W. T. In *Adhesion Science and Technology*; Lee, L. H., Ed.; Plenum Press: New York, 1975; Vol. 9a.
(11) Brown, H. R.; Deline, V. R.; Green, P. F. *Nature* **1989**, *341*, 221.

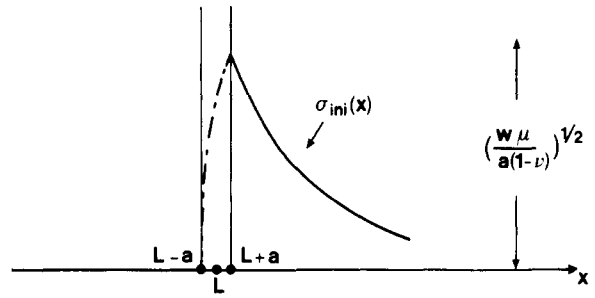

Figure 9. The normal stress $\sigma_{ini}(x)$ associated with the initiation distribution (A1.4).

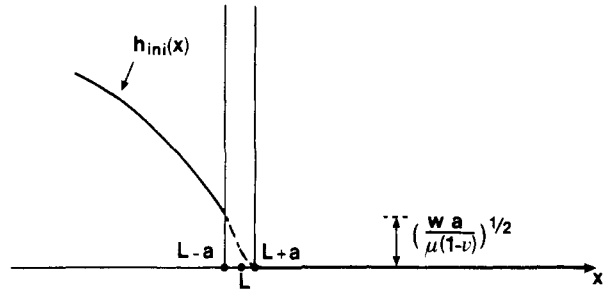

Figure 10. The crack opening $h_{ini}(x)$ associated with the initiation distribution (A1.4).

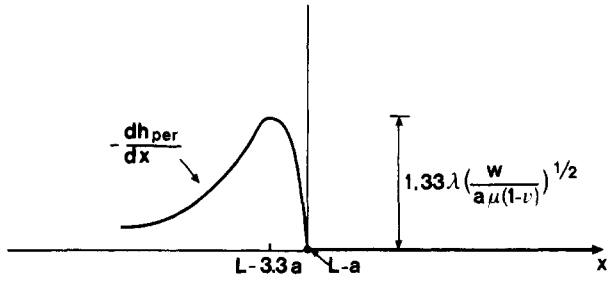

Figure 11. The density of dislocations $-dh_{per}/dx$ associated with the perturbative distribution (A2.4).

to be valid since the elongation ratio δ reaches its maximum value $\delta_{max} \simeq N_e^{1/2}$:

$$x_{min} - L \approx \frac{K^2}{(\mu\delta_{max})^2} \approx a\frac{a^2W}{kT} \qquad \text{(A1.3)}$$

If we assume that $W = \gamma_A + \gamma_B - \gamma_{AB} < kT/a^2$ (in accordance with our previous assumption $\gamma_A < kT/a^2$ (see section II.1), and with the fact that $\gamma_A \sim \gamma_B$), then $x_{min} - L$ is smaller than the monomer size a. We may then describe the elastic field associated with the junction by a distribution of sources (which we call the "initiation distribution")

$$\phi_{ini}(x) \simeq \begin{cases} \left(\frac{W}{\mu a^2(1-\nu)}\right)^{1/2} & (L-a<x<L+a) \\ 0 \quad \text{(otherwise)} \end{cases} \qquad \text{(A1.4)}$$

The associated normal stress ($\sigma_{ini}(x)$) and crack opening ($h_{ini}(x)$) are represented on Figures 9 and 10.

Appendix 2. The Perturbative Distribution

In order to check whether the result (eq 3.20)

$$\mu^{-1}\sigma_{per}(x) \simeq \lambda\left(\frac{W}{\mu(1-\nu)}\right)^{1/2}(L-x)^{-1/2} \qquad (0<x<L-a) \qquad \text{(A2.1)}$$

is consistent with the initial assumption (eq 3.19)

$$-\frac{dh_{per}}{dx} \ll -\frac{dh_{ini}}{dx} \qquad \text{(A2.2)}$$

we now examine the perturbative distribution of sources $\phi_{per}(x)$. According to eq A2.1, this function must satisfy

$$\int_0^x dy\ \phi_{per}(y)(x-y)^{-1/2} \simeq \lambda\left(\frac{W}{\mu(1-\nu)}\right)^{1/2}(L-x)^{-1/2} \qquad (0<x<L-a) \qquad \text{(A2.3)}$$

An approximate solution to eq A2.3 is given by

$$\phi_{per}(x) \simeq \begin{cases} \lambda\left(\frac{W}{\mu(1-\nu)}\right)^{1/2}(L-x)^{-1} & (0<x<L-a) \\ 0 \quad \text{(otherwise)} \end{cases} \qquad \text{(A2.4)}$$

(note that this solution would require some refinements for $x \sim 0$). The corresponding "density of dislocation" $-dh_{per}/dx$ is given by

$$-\frac{dh_{per}}{dx} = (1-\nu)\int_x^L dy\ \phi_{per}(y)(y-x)^{-1/2} \qquad \text{(A2.5)}$$

Its aspect is shown on Figure 11. The function $-dh_{per}/dx$ is maximal for $x \simeq L - 3.3a$:

$$\max_{(0,L-a)} -\frac{dh_{per}}{dx} = -\left.\frac{dh_{per}}{dx}\right|_{x\simeq L-3.3a} \simeq 1.33\lambda\left(\frac{W}{a\mu(1-\nu)}\right)^{1/2} \qquad \text{(A2.6)}$$

Remembering that (see Appendix 1)

$$\max_{(0,L-a)} -\frac{dh_{ini}}{dx} = -\left.\frac{dh_{ini}}{dx}\right|_{x\simeq L-a} \simeq \left(\frac{W}{a\mu(1-\nu)}\right)^{1/2} \qquad \text{(A2.7)}$$

we may write

$$\max_{(0,L-a)} -\frac{dh_{per}}{dx} \sim \lambda \max_{(0,L-a)} \frac{dh_{ini}}{dx} \qquad \text{(A2.8)}$$

Since in the slow regime λ satisfies $\lambda \ll 1$, we therefore conclude that the initial assumption (A2.2) is indeed satisfied.